

LA-UR-80-1109

TITLE: MEASUREMENTS OF ELECTRON HEAT FLOW ALONG A DC MAGNETIC FIELD
IN STRONG TEMPERATURE GRADIENTS

AUTHOR(S): R. S. Massey, J. C. Ingraham, B. L. Wright, H. Dreier

SUBMITTED TO: International Symposium on Open-Ended Fusion Systems,
Touluba, Japan
April 15-18, 1980

MASTER

By acceptance of this article, the publisher recognizes that the
U.S. Government retains a nonexclusive, royalty-free license
to publish or reproduce the published form of the contribu-
tion, or to allow others to do so, for U.S. Government pur-
poses.

The Los Alamos Scientific Laboratory requests that the pub-
lisher identify the article as work performed under the aus-
pices of the U.S. Government of Energy.

DISTRIBUTION STATEMENT



LOS ALAMOS SCIENTIFIC LABORATORY

Post Office Box 16633 Los Alamos, New Mexico 87545

An Affirmative Action Equal Opportunity Employer

MEASUREMENTS OF ELECTRON HEAT FLOW ALONG A DC
MAGNETIC FIELD IN STRONG TEMPERATURE GRADIENTS*

R. S. Massey, J. C. Ingraham, B. L. Wright, and H. Dreicer,
Los Alamos Scientific Laboratory, University of California,
P. O. Box 1663, MS650, Los Alamos, NM 87545, U. S. A.

ABSTRACT

Measurements of electron heat flow parallel to \vec{B} are performed on a fully-
confined plasma column under conditions for which the electron-electron
collisional mean free path, ℓ_{ee} , is not small relative to the electron
temperature-gradient scale-length, $|(1/T)(dT/dx)|^{-1}$. Pulsed microwave heating
at one location on the column and nonperturbing microwave resonator measurements
of temperature at two locations on the column are used to create and to measure
the heat flow. We compare our results with the predictions of a 1-D heat
diffusion code that has a parameter, α , multiplying the Spitzer heat
conductivity coefficient, and that also has provision for limiting the heat flux
to $q_L = \beta n k T \sqrt{kT/m}$ (where β is an adjustable parameter) in order to model the
transition to larger values of $(\ell_{ee}/T)|dT/dx|$. For a weak heating case
($T/T_0 \leq 1.25$, $(\ell_{ee}/T)|dT/dx| \sim 0.015$) we find $\alpha = 1.1 \pm 0.1$ gives best agreement
between measurements and predictions. For a strong heating case ($T/T_0 \sim 5$,
 $(\ell_{ee}/T)|dT/dx| \lesssim 0.7$) we find, using an α -value ≈ 1.1 , that a β -value of 0.25 is
required to give a good fit to the data.

I. Introduction

The rate of electron heat transport along magnetic lines is of fundamental
importance to the end loss problem of open-ended fusion systems. It also plays
a key role in the heat transfer within a device between regions of different
temperature, such as the end cell and center cell regions of a Tandem Mirror.
Though the rate of electron heat transfer is thought to be well-understood when
electron collisions dominate,¹ there exists no rigorously-derived theory that
describes electron heat transfer under conditions where electron collisions are
present but not dominant, or when strong temperature gradients exist. In this
weakly-collisional regime the ratio of the electron-electron collisional
mean-free-path to the temperature-gradient scale length, $\frac{\ell_{ee}}{T} \left| \frac{dT}{dx} \right| = \lambda$, is not
much less than unity. (Here, $\ell_{ee} = v_e \sqrt{kT/m}$, where v_e is given by Spitzer.²)
We present heat flow measurements that span the collision-dominated and
weakly-collisional regimes, and compare our results with the predictions of two
existing heat flow models.

II. Experimental Method

Using high-Q microwave resonators (heater and sensor) we perform non-perturbing measurements of electron temperature, T , in a study of electron heat flow along the fully-ionized plasma column of a single-ended potassium Q-machine (Fig. 1). The resonators operate in the TM_{010} mode ($f \approx 2$ GHz) with \vec{E}_{KF} parallel to the dc magnetic field, $\vec{B} \approx 4$ kG, $Q \approx 20,000$, and $\omega > \omega_p$. The plasma column is 183 cm long, the ambient electron and ion temperatures are assumed equal to the hot plate temperature (2250 K), and typical electron densities are $n \approx 4 \times 10^{10} \text{ cm}^{-3}$. Langmuir probes (P1, P2, P3) are located at three positions along the plasma column. The heat flow is caused by application of a brief localized microwave heating pulse using the heater resonator. The negatively-biased cold plate acts as an insulator to the heat flow and the hot plate is in good thermal contact with the plasma. The temperature measurement is based on the $T^{-3/2}$ dependence of the weak-field ac resistivity³ of a fully-ionized plasma as applied to resonator measurements of the plasma resistivity. The weak temperature dependence of the ac resistivity equal to logarithm term, $\ln \Lambda$, as given by Dawson and Oberman,³ is also included in the analysis. (In an earlier publication⁴ we reported experimental measurements of the plasma ac resistivity that were in good agreement with the Dawson-Oberman theory.)

We determine the plasma ac resistivity from a measurement of the rate of absorption by the plasma of microwave energy stored in the resonator. The rate of energy absorption in the resonator is determined directly from the decay rate of the electromagnetic energy following excitation of the resonant field. The plasma energy absorption rate is determined quantitatively from the difference between the measured energy decay rate in the presence of plasma, and the measured energy decay rate in the absence of plasma. Using a similar measurement for the unheated plasma and taking the ratio of the two plasma resistivities, we get in the ratio of the heated to unheated plasma temperatures.

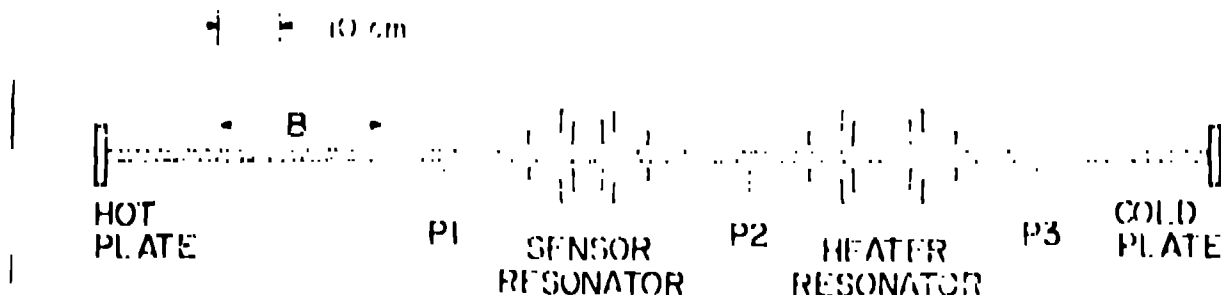


Fig. 1. Experimental arrangement for heat flow measurements on the single-ended Q-machine.

The resonator energy decay is measured in the following way. The decay of a signal proportional to the resonator energy is digitized using a Tektronix 7912 transient digitizer and the data transmitted to a computer. Through careful calibration procedures and analysis of error we have achieved an accuracy of better than 1% in the determination of the decay rate. Such resistivity temperature measurements are performed at the sensor resonator during and after application of the heating pulse by the heater resonator, and at the heater resonator after the heating fields have decayed to a sufficiently low level so that weak-field resistivity measurements can be made.

We compare our measurements with the predictions of computer solutions to the one-dimensional electron heat-flow equation:

$$\frac{3nk}{2} \frac{\partial T}{\partial t} = - \frac{\partial}{\partial x} q + H_0 F(t) S(x)$$

where q is the electron heat flux, and H_0 is the heater strength. $S(x)$ (Fig. 2) is the heater spatial dependence and is determined from a computer code⁴ that calculates the resonator field distribution in the presence of the plasma and the resonator end-holes. $F(t)$ (Fig. 2) is the heater time dependence and is determined by direct measurement of the rate of power absorption by the plasma during the heating pulse using the same technique as is used for the ac resistivity measurement. The electron density is determined from resonator frequency shifts and probe-measured radial electron density profiles.

For collision-dominated heat flow, $q = q_c = - \alpha \frac{\partial T}{\partial x}$, where α is the electron thermal conductivity,¹ and α an adjustable coefficient. To analyze cases where strong temperature gradients or long electron mean-free-paths occur we use the phenomenological flux limit expression⁶ $q = q_c / (1 + \frac{q_c}{q_L})$, which limits q to the limiting heat flux, q_L . In order to model the transition from collisional to collisionless heat transport, q_L is assumed to have the form of the collisionless heat transport rate, $q_L = FnkT \sqrt{\frac{kT}{m}}$, where F is an adjustable parameter. Typically, a value of F of about 0.6 has been used by others⁶ in attempting to predict heat flow in the weakly collisional regime.

Because n and T vary with radius, the effective temperature measured by a resonator, T_{eff} , is determined from an average over the profile of the quantity $n^2 \ln \Lambda / T^{3/2}$. In order to compute this average from the predictions of our one-dimensional heat-flow code, probe measurements of the n and T radial profiles at a single time are used (see Fig. 3). [The probe (P3) chosen for the

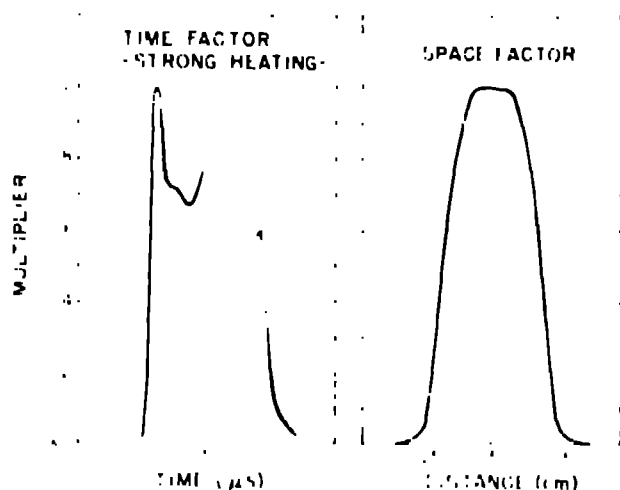


Fig. 2. Time and space factors for heating term in heat flow equation.

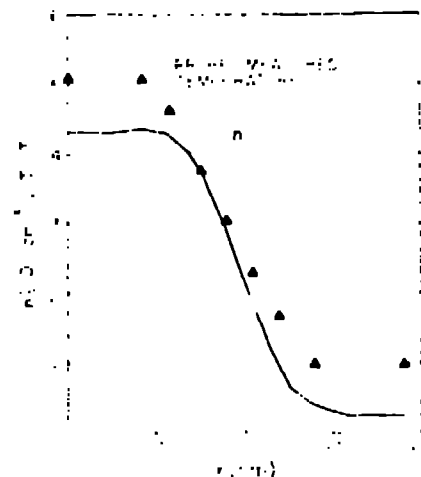


Fig. 3. Density and temperature profiles. Temperature measured 20.2 μ s after start of heater pulse.

measurements is located near the insulating cold plate so as to minimize perturbations on heat flow from the heater to the sensor.) The predictions of the heat flow code are fit to the probe measurements at a set of representative points on the profile by adjusting the value of H_0 at each point and are then combined in an integral over the plasma cross section of the quantity $n^2 q_0 \lambda / T^{3/2}$ to give a predicted $T_{\text{EPP}}(x, t)$ at the resonator positions. A similar integral is computed for the unheated plasma ($T = T_0$) to obtain T_{EPP}/T_0 for comparison with the resonator temperature measurements.

We determine β from the case of a weak heating pulse where collision-dominated heat transfer occurs. We determine β primarily from the case of a strong heating pulse where λ is no longer small. It is usually necessary to apply a small additional common correction ($< 20\%$) to all the H_0 -values for a given heating case in order to achieve the best fit to the temperature measurements. That such a correction should be necessary is not surprising in view of the uncertainties attached to Langmuir probe temperature measurements in a Q-machine plasma.

III. Experimental Results--Weak Heating

For the case of weak heating where the electrons are heated by bremsstrahlung absorption the temperature $T_{\text{EPP}}(\text{heater})$ is increased by about 30%, as can be seen in Fig. 4 by extrapolating back to the time of heater turnoff. The corresponding $T_{\text{EPP}}(\text{sensor})$ is shown in Fig. 5. The two curves shown on Figs. 4 and 5 are computer solutions of the heat flow equation with $\alpha = 1.15$, and differ only in that slightly different values of the heater strength are used for the curves so as to optimize the agreement between the code predictions and either the sensor or the heater T_{EPP} . Because of the much

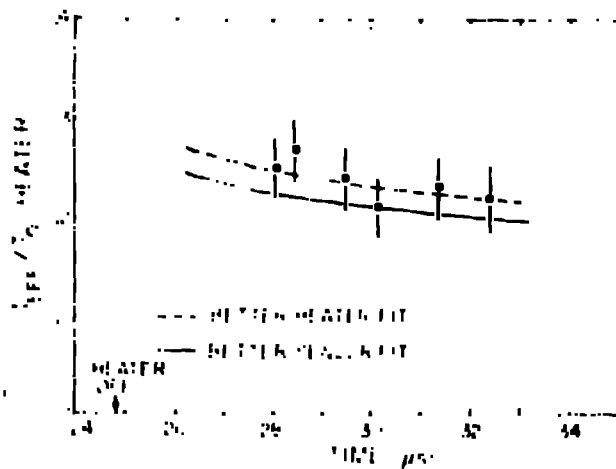


Fig. 4. Comparison at heater of heat heater fit with best sensor fit.

larger amount of data available at the sensor, we regard achieving a good fit with the sensor data as the more significant of the two possibilities. By comparison of the code and experiment for other α -values we have determined that the α -value providing the best fit to the data for this weak heating case is $\alpha = 1.1 \pm 0.1$, which constitutes a strong confirmation of the collision-dominated heat flow theory.¹ We have also verified that the heat flow code predictions for this weak heating case are not significantly

affected by the introduction into the code of a flux limit, $\beta = 0.25$ (which corresponds to the β -value determined in the next section). This is so in this case because $|q_c|$ is always much less than $|q_l|$.

Using the axial temperature distributions predicted by the heat-flow code at a representative radius on the profile (on half the electrons located at smaller radii), we have computed λ as a function of time and location on the column. We find that $\lambda \leq 0.015$ for this weak heating case.

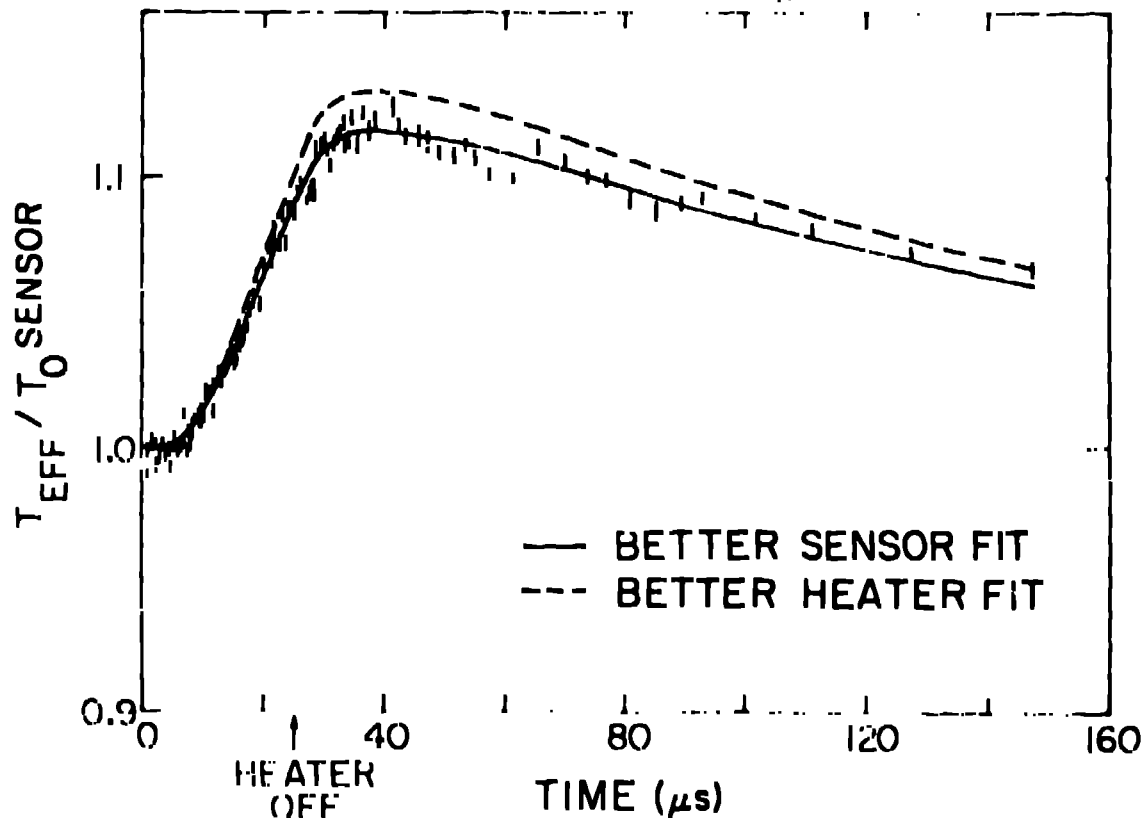


Fig. 5. Comparison at sensor of heat heater fit with best sensor fit.

IV. Experimental Results--Strong Heating

It is not possible to achieve strong heating of the electrons by relying solely on inverse bremsstrahlung absorption⁴ because the microwave heating rate of the plasma actually decreases with increasing microwave fields if the electron oscillating velocity is much larger than the electron thermal velocity. This decrease occurs because of the v^{-3} dependence of the coulomb collision rate. In addition to this field dependent effect, of course, the inverse bremsstrahlung heating becomes very inefficient at large T .

In order to achieve strong heating, it was thus necessary to rely on enhanced heating by parametric instabilities⁷ excited by operating the heater at power levels above the instability threshold. In this case $T_{\text{EFF}}(\text{heater})$ is increased by about a factor of five as inferred from Fig. 6. Figure 6 also shows the results of two heat flow code runs with $\alpha = 1.15$, and $\beta = 0.2$ and 0.3 ,

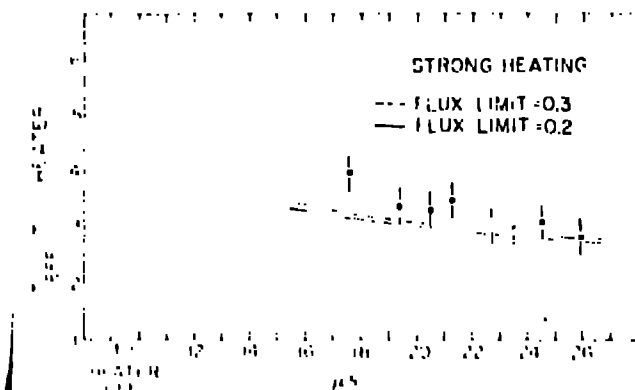


Fig. 6. Comparison at heater of best sensor fits for $\beta = 0.2$ and 0.3 .

respectively. The fit to the data for these two runs is optimized by comparison to $T_{\text{EFF}}(\text{sensor})$ as shown in Figs. 7 and 8 for early and late times, respectively. The peak value and later time decay of $T_{\text{EFF}}(\text{sensor})$ are well-bracketed by these two cases, suggesting $\beta \approx 0.25$ as a suitable optimum value for the fit to $T_{\text{EFF}}(\text{sensor})$. By carrying out heat flow code runs for several α and β values we

have determined that a $\pm 10\%$ uncertainty in the α -value determined in the weak-heating case gives rise to a $\pm 20\%$ uncertainty in β for the strong-heating case, $\beta = 0.25 \pm 0.05$. We have also found that for no flux limit ($\beta = \infty$) the peak value of $T_{\text{EFF}}(\text{sensor})$ can be satisfactorily predicted by the heat flow code using $\alpha = 0.2$, (that is, a factor of five reduction in the effective rate of diffusional heat transport), but that the predicted late time decay of $T_{\text{EFF}}(\text{sensor})$ is much too slow. Thus, the flux limiter model provides a much better overall fit to the data than does a model that adjusts only the size of the thermal conductivity coefficient.

The early time disagreement between the heat flow code predictions and $T_{\text{EFF}}(\text{sensor})$, where the data actually rises before the code predictions, was caused by hot nonthermal electrons in the tail of electron velocity distribution,⁷ which are produced as a result of the parametric instabilities. These nonthermal electrons have very long mean free paths and rapidly leave the plasma column at the hot plate after the heater pulse is terminated, leaving

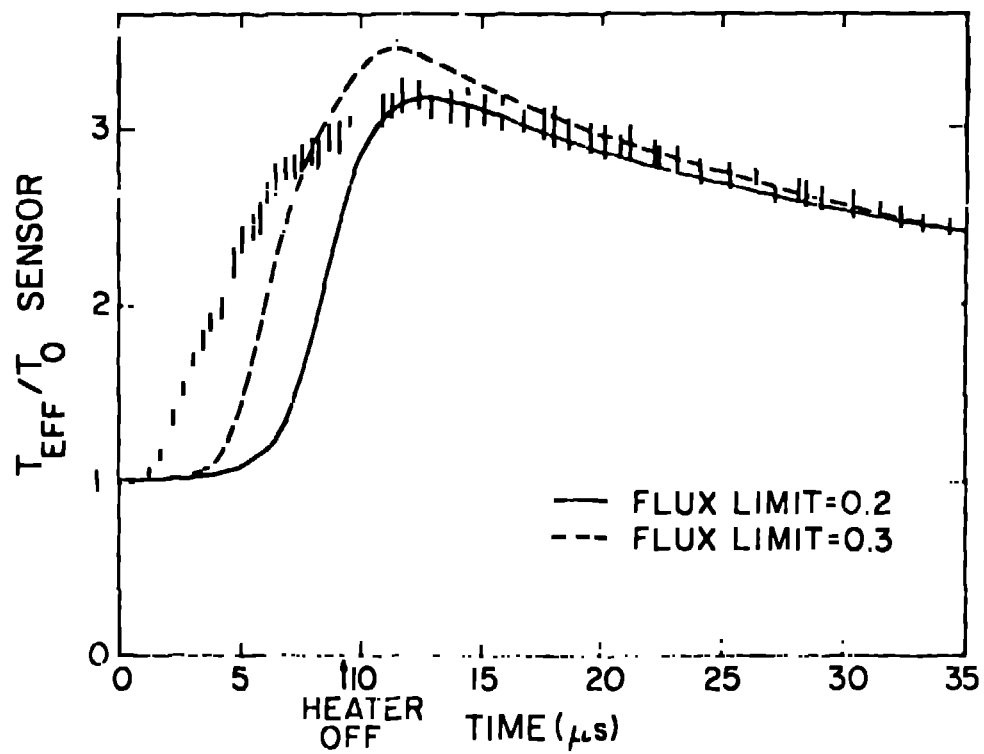


Fig. 7. Comparison at sensor of best sensor fits for $\beta = 0.2$ and 0.3 .

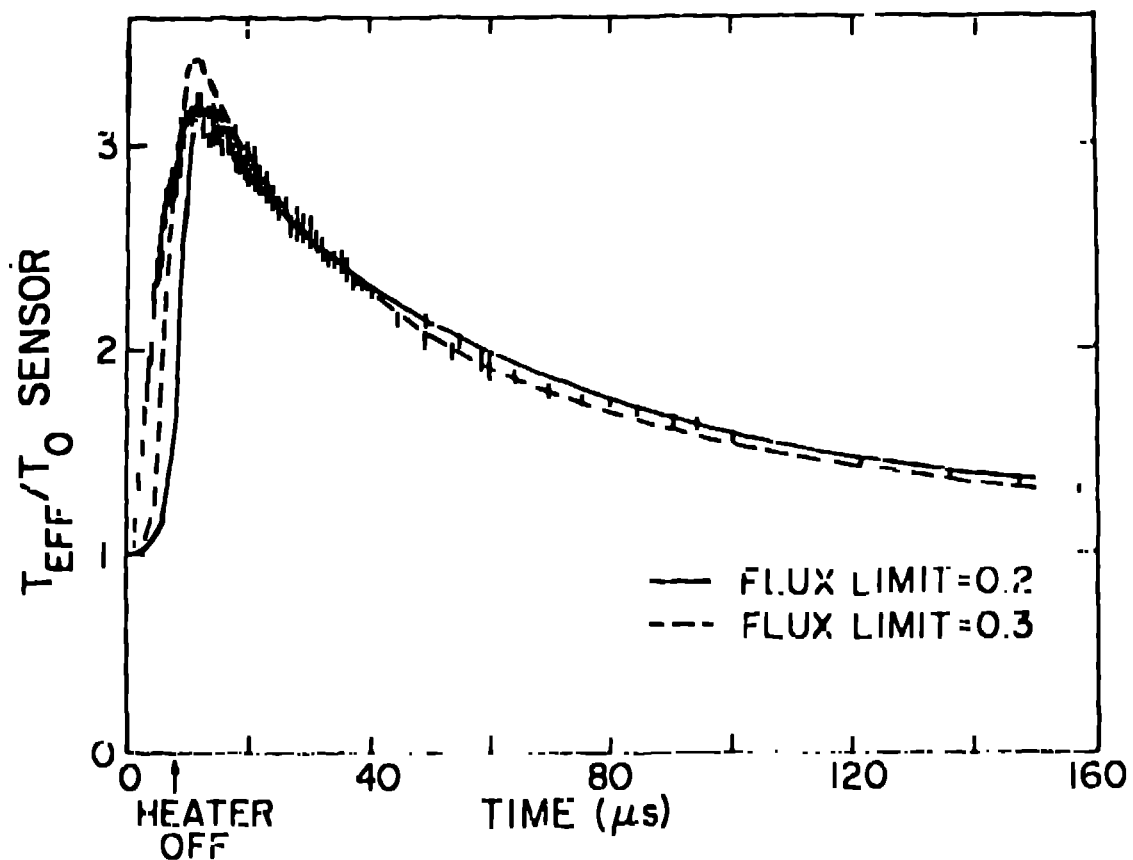


Fig. 8. Comparison at sensor of best sensor fits for $\beta = 0.2$ and 0.3 .

behind the strongly-heated but cooler body of the electron velocity distribution. The strongly-heated body then transports its heat along the plasma column at the slower rate described by the flux-limited heat flow model. For cases of strong heating by parametric instabilities we find a large difference between the measured absolute energy absorbed by the plasma and the amount of energy required to produce the temperatures that are ultimately measured. Estimates indicate that if this energy differential was carried rapidly out of the column by the hot nonthermal electrons, their density and velocities could have been sufficient to produce the observed early rise of $T_{\text{EFF}}(\text{sensor})$. (This rise occurs as a result of a reduction in the ac resistivity caused by the backflow velocity⁸ induced in the unheated electrons by the hot electrons.) On the other hand, for the weak heating case where only inverse bremsstrahlung absorption heats the electrons we obtain reasonable agreement between the measured and calculated absorbed energies.

Figure 9 shows a comparison with $T_{\text{EFF}}(\text{sensor})$ data of two additional heat flow code runs: $\alpha = 1.0$ and $\beta = \infty$; and $\alpha = 1.15$ and $\beta = 1.5$. It is apparent that such cases cannot provide good agreement with the data and would seriously overestimate the peak of $T_{\text{EFF}}(\text{sensor})$ if applied to this case. For the $\alpha = 1.0$ and $\beta = \infty$ case the predicted amount of energy required to heat the electrons is

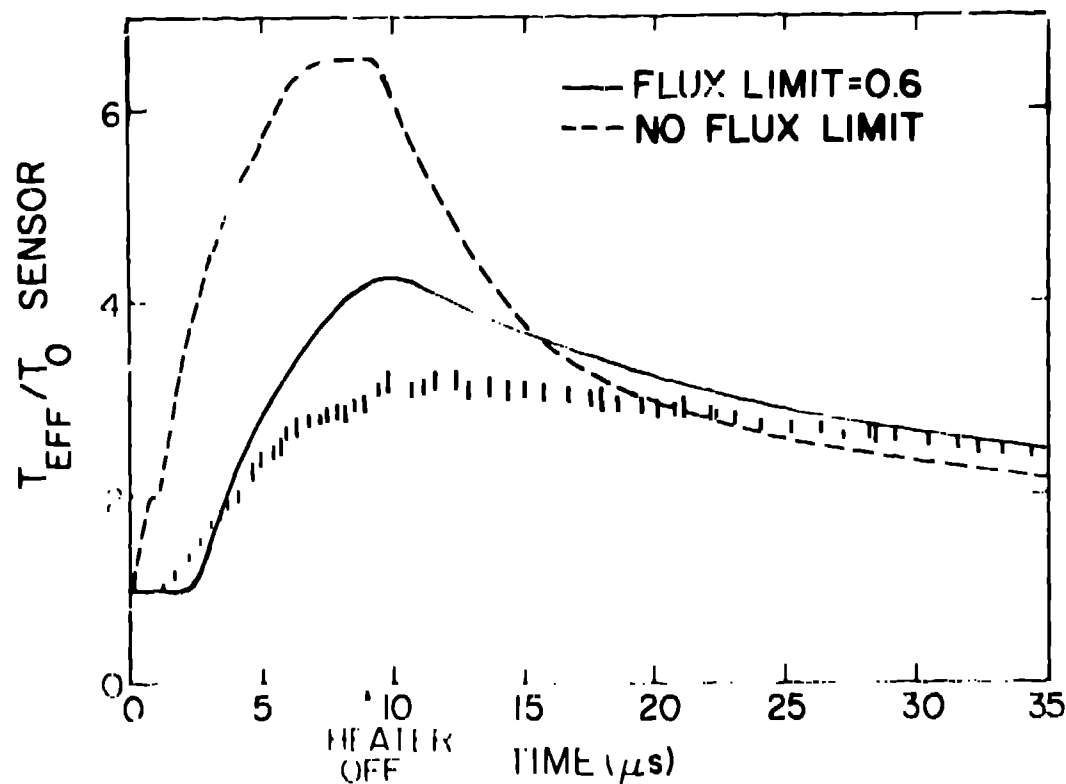


Fig. 9. Comparison at sensor of heat sensor fits for $\beta = 0.6$ and ∞ .

almost two orders of magnitude larger than the measured absorbed energy. This result further emphasizes the unphysical nature of the diffusion heat flow model predictions ($\beta = \infty$) for this strong heating case.

We have computed the values of the quantity λ that occur in this strong heating case from the heat flow code solution for $\alpha = 1.15$ and $\beta = 0.3$ at a representative radius on the column profile (one-half the electrons at smaller radii). The predicted values of λ rise as high as 0.7 during these early times when strong flux-limited behavior is observed but are less than 0.07 for later times ($> 45 \mu s$).

V. Discussion of Results and Conclusions

In the case of the weak heating pulse where $\lambda \lesssim 0.015$ our measurements have confirmed the collision-dominated heat flow theory¹ to within 10% ($\alpha = 1.1 \pm 0.1$).

In the strong heating case we found that a flux-limiting β -value of 0.25 was required to fit the peak and late time behavior of $T_{\text{eff}}(\text{sensor})$ when $\alpha = 1.15$ was assumed. We also found by computation that values of λ range from as high as 0.7 at early times to less than 0.07 at late times ($t \gtrsim 45 \mu s$). From the definition of the limited flux, $q = q_c / (1 + |q_c/q_L|)$, it is apparent that the flux-limit effect becomes predominant for $|q_c/q_L| > 1$. Expressing q_c/q_L in terms of λ and using $\alpha = 1.15$ and $\beta = 0.25$, we find that the flux-limit effect is predominant for $\lambda \gtrsim 0.1$, which provides a useful guideline for the limit of validity of the collision-dominated theory.

The experimentally-determined value of $\beta = 0.25$ is significantly less than the commonly-used value,⁶ $\beta = 0.6$. The best value of β to use in a particular experiment depends on the processes present that affect the heat flow. We have not yet carried out a systematic experimental search for plasma fluctuations^{9,10,11} that might be excited by the electron heat flux in the strong heating case, and which would act to retard the heat flow. However, rough estimates of the expected growth rates of these heat flux instabilities can be made by modelling our strong heat flux cases with a two-Maxwellian model,¹⁰ and these indicate that no heat flux instabilities should be excited. The possible role of the hot nonthermal electrons produced by parametric instability heating remains to be examined in more detail. If these electrons are of sufficient density they could excite two-stream instabilities with the background plasma electrons and ions, which could result in additional plasma heating as well as modifications to the heat flow by the resultant turbulence. A preliminary analysis of an intermediate heating case where both the heat flux and the hot nonthermal electron production is weaker indicates that a somewhat

larger value of β ($\approx 0.3-0.6$) provides a better fit to the data. This may suggest a role is being played by instabilities in the strong heating pulse case reported here.

VI. Acknowledgements

We are grateful to S. P. Gary and R. J. Mason for helpful discussions.

*Work performed under the auspices of the U.S. Department of Energy.

REFERENCES

1. R. Landshoff, Phys. Rev. 82, 442 (1951); L. Spitzer and R. Härm, Phys. Rev. 89, 977 (1953); S. I. Braginski, Rev. Plasma Phys. 1, 205 (1965).
2. L. Spitzer, "Physics of Fully-Ionized Gases," Interscience (1962), p. 133.
3. J. Dawson and C. Oberman, Phys. Fluids 5, 517 (1962).
4. J. H. Brownell, H. Dreicer, R. F. Ellis, and J. C. Ingraham, Phys. Rev. Lett. 33, 1210 (1974).
5. J. D. Thomas, to be published.
6. R. C. Malone, R. L. McCrory, and R. L. Morse, Phys. Rev. Lett. 34, 721 (1975); G. A. Moses and J. J. Duderstadt, Phys. Fluids 20, 762 (1977).
7. H. Dreicer, R. F. Ellis, and J. C. Ingraham, Phys. Rev. Lett. 31, 426 (1973).
8. T. Musha and F. Yoshida, Phys. Rev. 133, A1302 (1964); M. E. Banton, H. Dreicer, J. C. Ingraham, and B. L. Wright, Bull. Am. Phys. Soc. 22, 1160 (1977), and to be published.
9. W. M. Manheimer, Phys. Fluids 20, 265 (1977).
10. S. P. Gary, J. Plasma Phys 20, 47 (1978), and 21, 361 (1979).
11. A. Ramani and G. Laval, Phys. Fluids 21, 980 (1978).